

Evaluations of land/ocean skin temperatures of the ISCCP satellite retrievals and the NCEP and ERA reanalyses

Ben-Jei Tsuang (莊秉潔)^{1*}, Ming-Dah Chou², Yuanchong Zhang³, Andreas Roesch⁴, Kun Yang⁵

1: Department of Environmental Engineering, National Chung Hsing University, Taichung 402, Taiwan

2: Department of Atmospheric Sciences, National Taiwan University, Taipei 106, Taiwan

3: Columbia University at NASA GISS, 2880 Broadway, RM 320-B, New York, NY 10025, USA

4: Institute for Atmospheric and Climate Science, Universitätsstrasse 16 ETH Zentrum, CHN, CH-8092 Zürich, Switzerland

5: Department of Civil Engineering, The University of Tokyo, Tokyo, Japan

*: Corresponding author: Email: tsuang@nchu.edu.tw, Fax: +886-4-22862587, Tel: +886-4-22851206

Abstract

This study evaluates the skin temperature (ST) datasets of the ISCCP-D satellite product, the ISCCP-FD satellite product, the ERA40 reanalysis, the NCEP-NCAR reanalysis and the NCEP-DOE AMIP-II reanalysis. All the datasets are correlated to each other, with correlation coefficients of monthly anomalies > 0.50 . To evaluate their qualities, the 5 ST datasets are used to calculate clear-sky (CS) outgoing longwave radiation (OLR) and upward surface longwave radiation (USLR); the results are compared with the ERBE satellite observation (Figure 1 and Table 1) and 14 surface station (Figure 2). The satellite-derived STs and ERA40 ST tend to bias high on hot deserts (e.g., Sahara Desert), and the reanalyzed STs tend to bias low in mountain areas (e.g., Tibet). In northern-hemisphere high latitude regions (tundra, wetlands, deciduous needle-leaf forests and sea ice), the CS OLR anomalies calculated using the satellite-derived STs have higher correlations and lower root-mean-squared errors with the ERBE satellite observation than those derived from using the reanalyzed STs. ERA40 underestimates the amplitude of the seasonal ST over glaciers. All the reanalysis products (ERA40, NCEP-NCAR, NCEP-DOE AMIP-II) overestimate the ST during partial sea-ice-covered periods in the middle-high latitude oceans. Nonetheless, suspected spurious noises with an amplitude of 2 K in the satellite-derived STs produce a physically unviable anomaly over Earth surface where the amplitude of the anomaly is weak (such as open water bodies, croplands, rainforest, grasslands, hot deserts, cold deserts).

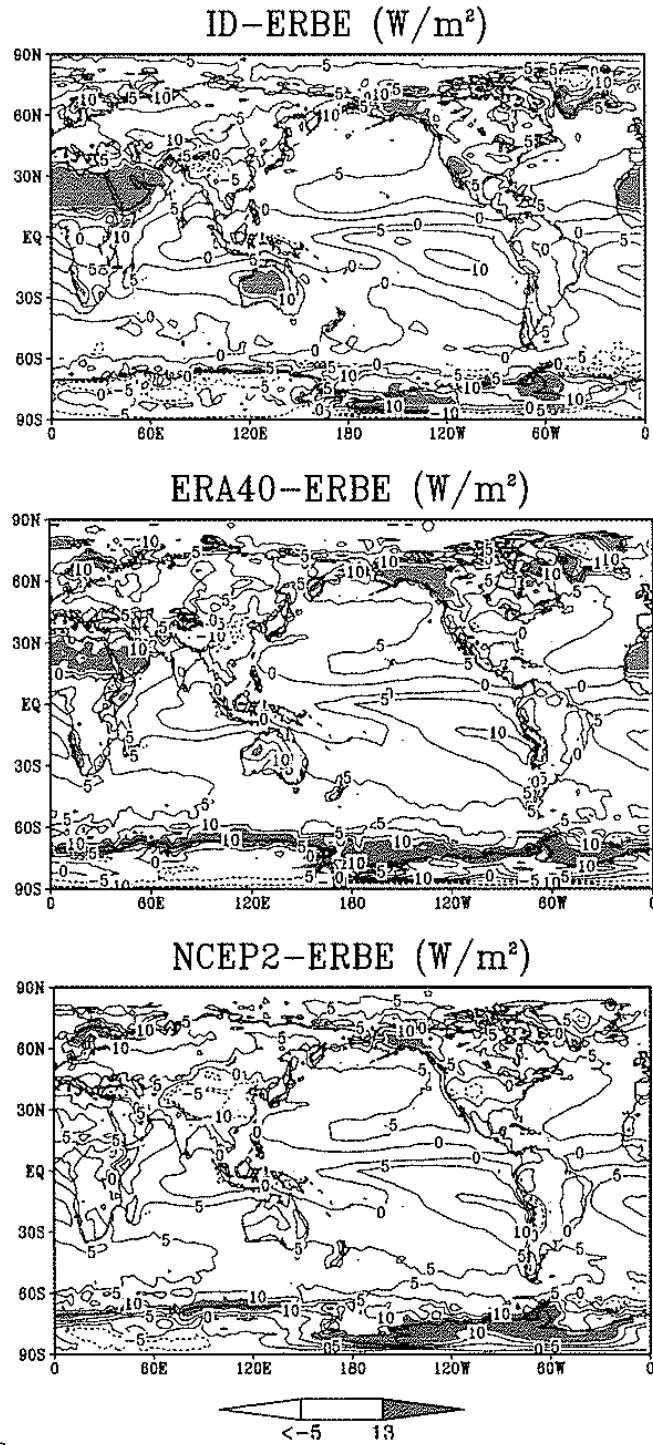


Figure 1 Bias ($W m^{-2}$) of the simulated CS OLRs compared with ERBE during 1985-1989, where regions with bias > 3 standard deviation are shaded (i.e., $> 13 W m^{-2}$ or $< -5 W m^{-2}$). Note that the CS OLR modeling system of this study systematically biases high by $4 W m^{-2}$ with the standard deviation at $3 W m^{-2}$.

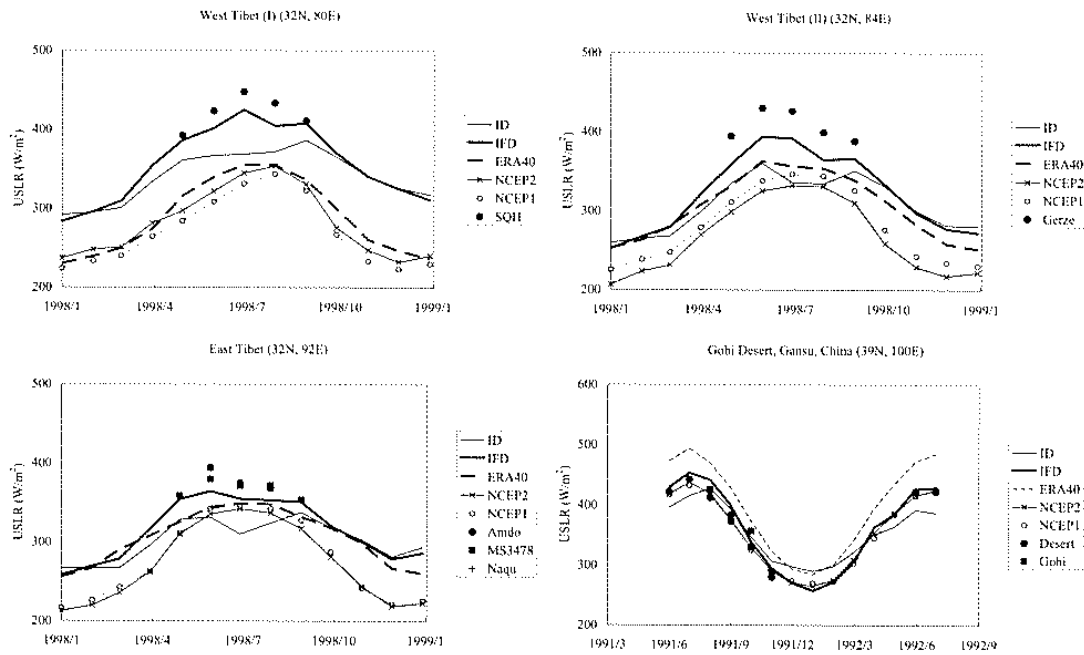


Figure 2 Time series of upward surface longwave radiations (USLR) in Tibet and Gobi desert, as simulated using the skin temperatures of ID, IFD, ERA40, NCEP2 and NCEP1.

Table 1 Biases of the simulated CS OLRs (W m^{-2}) of ID, IFD, ERA40, NCEP2 and NCEP1 runs, and the original ERA40 dataset (Simmons and Gibson, 2000) compared with ERBE.

Land type	Grid number	ID	IFD	ERA40	NCEP2	NCEP1	org. ERA40
Glacier	59	6.8	9.9	8.3	8.7	7.1	3.8
Wetlands	16	7.5	10.9	8.1	6.5	6.4	2.8
Open water	4,461	3.0	3.3	3.7	3.6	3.7	-0.6
Croplands	381	3.5	3.6	2.2	1.2	0.8	-3.2
Other forests	333	5.8	6.8	5.7	4.5	3.7	0.7
Rainforest	198	0.3	0.4	1.9	1.5	1.1	-1.6
Deciduous needle-leaf forests	39	4.4	6.4	5.5	3.6	2.6	-0.2
Grasslands	336	5.3	5.8	2.6	0.8	0.6	-2.6
Tundra	210	8.5	12.2	9.2	6.9	6.3	3.7
Cold desert	92	8.0	8.1	2.8	-1.3	-2.3	-3.8
Hot desert	345	17.4	15.9	11.4	5.8	7.5	3.8
Ocean with ice >0 but ≤10%	310	3.1	4.0	5.9	5.3	5.4	1.2
Ocean with ice >10%	637	6.3	7.5	8.0	4.6	4.1	3.5
Tibet	8	2.4	0.4	-10.2	-13.9	-17.8	-16.1
Mountain Andes	2	-0.1	2.8	-13.6	-11.3	-13.1	-13.0